

Nonlinear control of structure using neuro-predictive algorithm

Amir Baghban, Abbas Karamodin* and Hasan Haji-Kazemi

Department of Civil Engineering, Ferdowsi University of Mashhad, Iran

(Received March 18, 2014, Revised December 2, 2015, Accepted December 5, 2015)

Abstract. A new neural network (NN) predictive controller (NNPC) algorithm has been developed and tested in the computer simulation of active control of a nonlinear structure. In the present method an NN is used as a predictor. This NN has been trained to predict the future response of the structure to determine the control forces. These control forces are calculated by minimizing the difference between the predicted and desired responses via a numerical minimization algorithm. Since the NNPC is very time consuming and not suitable for real-time control, it is then used to train an NN controller. To consider the effectiveness of the controller on probability of damage, fragility curves are generated. The approach is validated by using simulated response of a 3 story nonlinear benchmark building excited by several historical earthquake records. The simulation results are then compared with a linear quadratic Gaussian (LQG) active controller. The results indicate that the proposed algorithm is completely effective in relative displacement reduction.

Keywords: structural control; active controller; neural network controller; neuro-predictive algorithm; model predictive control (MPC); fragility curves

1. Introduction

With the increasing progress in the field of structural control, various control methods have been proposed. Generally, these methods can be divided in two groups. The first group includes control methods which require a mathematical model of the system to operate (Gholampour *et al.* 2014, Suhir 2014, Zhang *et al.* 2008). Although structural models can be developed, there are many sources of uncertainty, measurement noise and nonlinearity that result in less-effective control algorithms. LQR, LQG, H2 and sliding mode control methods are some examples of this group. The second group includes control methods which do not require an accurate mathematical model of the system (Reigles and Symans 2006, Pourzeynali *et al.* 2007, Lu *et al.* 2010, Karamodin *et al.* 2012). They are based on the actual measured responses of the system and are therefore, referred to as nonmodel-based control methods. Fuzzy and neural network control methods are some examples of this group.

Model predictive control (MPC) belongs to a class of algorithms which compute a sequence of manipulated variable adjustment to optimize the future behavior of a plant. A state model is utilized to predict the open-loop future behavior of the system over a finite time horizon from present states. The predicted behavior is then employed to find a finite sequence of control actions that minimizes a particular cost function within pre-specified constraints. MPC displays its

*Corresponding author, Professor, E-mail: a-karam@um.ac.ir

effectiveness in its computational expediency, treatment of constraints, real-time applications, intrinsic compensation for time delays, and potential for future extensions of the methodology. The MPC scheme has been commonly utilized for the control of chemical processes and applications to automotive and aerospace industries (Qin and Badgwell 1996, Camacho and Bordons 1999). Rodellar *et al.* (1987) and Lopez- Almansa *et al.* (1994a, b) applied a special case of MPC that is a predictive control scheme in civil engineering studies. Other applications of MPC to the control of civil engineering structures have been demonstrated by Mei *et al.* (2001, 2002), Karamodin and Kazemi (2008) and Kim *et al.* (2013).

MPCs can be divided in two groups: linear and nonlinear. Linear MPC refers to a family of MPC schemes in which linear models are used to predict the system dynamics, even though the dynamics of the closed-loop system is nonlinear. Many systems are, however, in general inherently nonlinear. In these cases, linear models are often inadequate to describe the process dynamics and nonlinear models have to be used. This motivates the use of nonlinear model predictive control.

Developing nonlinear model of complex systems is difficult. One method to do that is artificial neural networks (ANNs). The ANNs have been proven to be useful for solving certain types of problems that are nonlinear, complex and poorly understood. This type of network has been found to be a powerful computational tool for organizing and correlating information. The applications of ANNs to the area of structural control have been used through controller replication, system identification, or system inverse identification (Jung *et al.* 2004, Bani-Hani *et al.* 2006, Lee *et al.* 2006, Kumar *et al.* 2007)

In this paper active neural network predictive controller (NNPC) is used to control nonlinear structures subjected to ground excitations. A neural network model of nonlinear structure predicts future structural response. The controller then calculates the control input that will optimize a cost function over a specified future time horizon. Since the NNPC is very time consuming and not suitable for real-time control, NNPC is used to generate the training data for a neural network (NN) controller. The effectiveness of the NNPC and NN controllers are illustrated and verified using simulated response of a 3-story full-scale, nonlinear benchmark building excited by several historical earthquake records. Fragility curves are generated to show the reduction in probability of damage. The performance of this algorithm is compared with the LQG controller.

2. MPC scheme

MPC is based on iterative, finite horizon optimization of a plant model. At each consecutive sampling instant k the current plant state is sampled and a cost minimizing control strategy is computed for a relatively short time horizon in the future. The optimization cost includes minimization of the difference between the predicted and desired responses and the control effort subject to prescribed constraints such as limits on the magnitude of the control force. In the MPC scheme, first a reference response trajectory $y_r(k)$ is specified. The reference trajectory is the desired target trajectory of the structural response. This is followed by an appropriate prediction model, which is then used to estimate the future structural response $y(k)$. The prediction is made over a pre-established extended time horizon using the current time as the prediction origin. The general principle of predictive control is as follows: at each consecutive sampling instant k , the control inputs $u(k) = u(k/k)$, $u(k+1/k)$, \dots , $u(k+\lambda-1/k)$ are calculated, assuming $u(k+n/k) = u(k+\lambda-1/k)$ for $n \geq \lambda$, where λ is the *control horizon*. The applied notation ' $u(k+n/k)$ ' means the prediction of the control input value for the future time $k+n$, performed at the time k . The control

inputs are calculated in such a way as to minimize differences between the predicted controlled outputs $\hat{y}(k+n/k)$ and the desired outputs $y_r(k+p/k)$ over the *prediction horizon* p ($n = 1, 2, \dots, p$). Then, only the first element $u(k/k)$ of the calculated sequence is applied to the structure, i.e., $u(k) = u(k/k)$. At the next sample ($k+1$), there occurs a new measurement of the process outputs and the whole procedure is repeated, with the prediction horizon of the same length p , but shifted by one step forward. Fig. 1 describes schematically the basic MPC scheme.

Determination of the control input trajectory over the control horizon is realized in the predictive algorithms on the basis of a model, by minimizing a cost function describing the control quality over the prediction horizon. A prime component of this function is the cost of deviations of the predicted outputs from the set points, i.e., the cost of predicted control errors. Moreover, it is also typical to include into the cost function, penalties on control changes. Regarding the two components, the following most commonly used quadratic cost function can be formulated

$$J = \sum_{j=1}^p (y_r(t) - \hat{y}(t+j))^2 + \rho \sum_{j=1}^{\lambda} (\hat{u}(t+j-1) - \hat{u}(t+j-2))^2 \tag{1}$$

where p and λ define the prediction and control horizons, respectively. The \hat{u} variable is the tentative control signal, y_r is the desired response, and \hat{y} is the network model response. The ρ value determines the contribution that the sum of the squares of the control increments has on the performance index.

3. Three-story benchmark building

The representative structure employed in this study is the SAC 3 story nonlinear benchmark building. The structure is designed for the Los Angeles, California area and defined by Ohtori *et al.* (2004). It's 36.58 m by 54.87 m in plan, and 11.89 m in elevation, Fig. 2. The bays are 9.15 m on center, in both directions, with four bays in the north-south (N-S) direction and six bays in the east-west (E-W) direction.

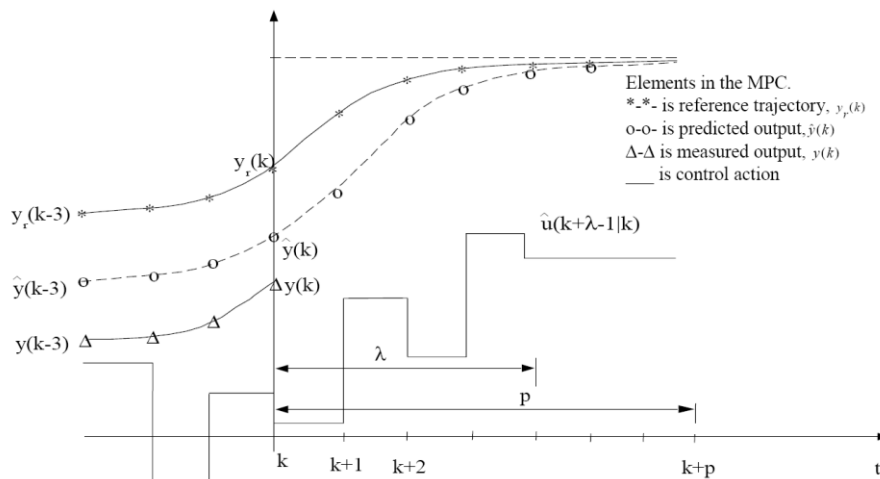


Fig. 1 MPC scheme

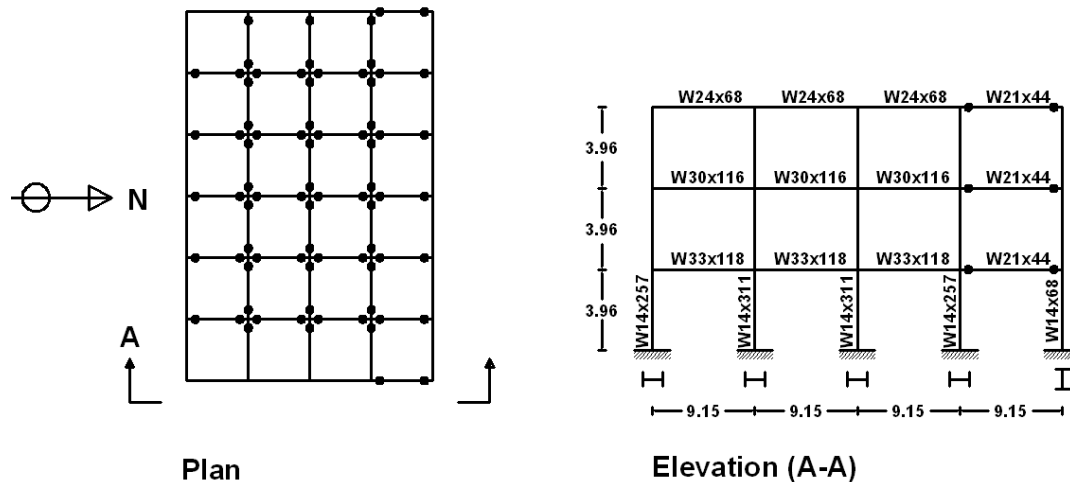


Fig. 2 Plan and elevation of 3 story nonlinear benchmark building

The building's lateral load-resisting system is comprised of steel perimeter moment-resisting frames (MRFs) with simple framing between the two furthest south E-W frames. The interior bays of the structure contain simple framing with composite floors. The floor system is assumed to be rigid in the horizontal plane. Since the building is quite regular in plan and elevation, only half of the building is considered for further analysis. The MRF to be analyzed is one of the two in the North-South direction and was assigned half the seismic mass of the whole structure. The first, second and third periods of frame are 1.01, 0.33 and 0.17 s, respectively.

Three sensors for displacement measurements system on the first, second, and third floors of structure and one sensor for ground acceleration measurement are used for feedback in the control system. During large seismic events, structural members can yield, resulting in nonlinear response behavior that may be significantly different than a linear approximation. To represent the nonlinear behavior, a bilinear hysteresis model is used to model the plastic hinges. These plastic hinges, which are assumed to occur at the moment resisting column-beam and column-column connections, introduce a material nonlinear behavior of structures.

4. Proposed control strategy

4.1 Neural network predictive controller

Fig. 3 illustrates the proposed control strategy. The required control force is calculated by an NNPC algorithm, which is based on MPC scheme. NNPC consists of a neural network model of structure and a numerical optimization algorithm. Basically there is no limitation on choosing response for control, but because here the three story structure is used for simulation and for short structure relative displacement can be the most important criteria, this response is selected for control. The neural network model is used to predict the open-loop future behavior of the story

over a finite time horizon from present states. Here, one controller is used for each story to control relative displacement of the story. The input to the neural network model is the relative displacement of story and ground acceleration. The ground acceleration is assumed to be constant over the horizon. The output of the neural network is the predicted relative displacement of story, which is then sent to the optimization algorithm to find a finite sequence of control actions, which minimizes the cost function (Eq. (1)) within pre-specified constraints. Here, p , λ and ρ are selected 5, 5 and 0.005, respectively.

As discussed above, the NNPC proposed in this paper requires a neural network model of structure. This NN model calculates the relative displacement of story based on the current and few previous histories of relative displacement, ground acceleration, and control force. To train the NN, the band limited white Gaussian noise is used to generate randomly control force and Elcentro records is used to generate data as ground acceleration (Fig. 4). Relative displacement of stories due to these ground acceleration and control forces are calculated considering nonlinear material behavior described by Ohtori *et al.* (2004) and briefly presented in this paper. The sampling rate of the training data was 100 Hz for 30s period, which resulted in 3000 patterns for training, testing, and validation. To select the network architecture, it is required to determine the numbers of inputs, outputs, hidden layers, and nodes in the hidden layers which is usually done by trial and error. The most suitable input data in our case were found to be the current and the two previous histories for the relative displacement, ground acceleration and control force. In addition, one hidden layer, with fifteen nodes, was adopted as one of the best suitable topologies for the NN. The tansig activation function is used for the hidden layer and the linear function for the output layer, which represents the control force.

4.2 Neural network controller

As stated earlier, the NNPC controller should minimize a performance index at each time step to find the required force in order to produce the desired response. This minimization is very time consuming and is not suitable for real-time control of system subjected to seismic excitations. So, The NNPC is used to train a single neural network that works as a standalone controller. This NN controller estimates the control force from the feedback sensors directly.

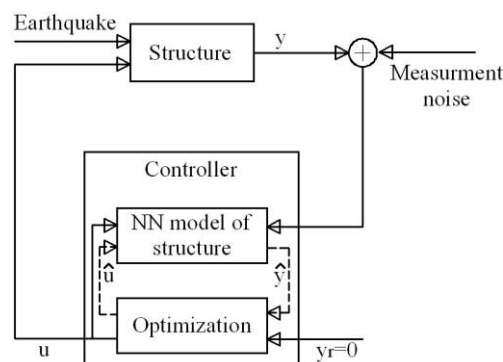


Fig. 3 Proposed control strategy

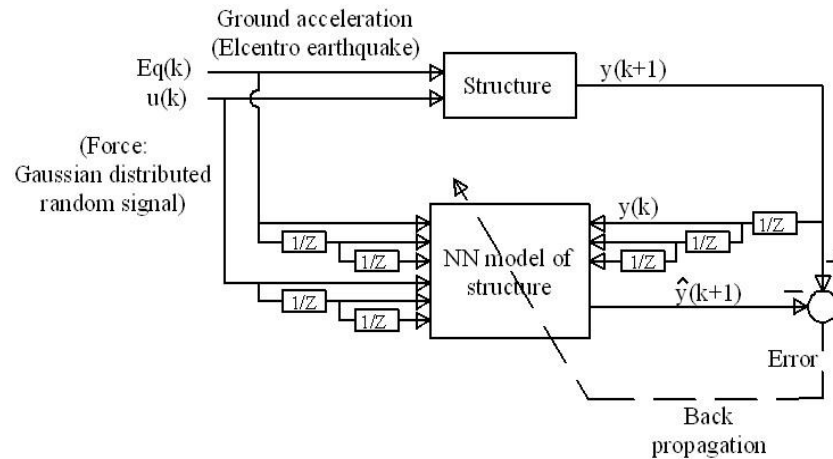


Fig. 4 Training NN model of structure

One controller is trained for each story. Training these NN controllers are performed offline by generating the required training patterns when the structure is excited by 40 s of the El Centro earthquake record and controlled by the NNPC controllers. The data used to train these controllers are prepared as depicted in Fig. 5. The sampling rate is 200 Hz and the training patterns numbered 8000. The network architecture was designed to have 9 input neurons representing the current and two previous histories of the ground acceleration, relative displacement of story and control force. One hidden layer having 20 hidden neurons was selected by trial and error. Finally, the output layer has one neuron, representing the control force of each story. The tansig activation function was used for the hidden layer and linear was used for the output layer (control force).

5. Control performance

To investigate the effectiveness of the control system, two groups of criteria are selected. The first includes criteria are proposed in nonlinear benchmark problem defined by Ohtori *et al.* (2004) to evaluate interstory drift ratio, story acceleration and base shear. The second is fragility curves. The fragility curves show the probability of structural damages as a function of ground motion intensity.

5.1 Benchmark problem criteria

In the benchmark problem, two far-field and two near-field historical ground motion records are proposed: (1) El Centro. The N-S component recorded at the Imperial Valley Irrigation District substation in El Centro, California, during the Imperial Valley, California earthquake of May 18, 1940. (2) Hachinohe. The N-S component recorded at Hachinohe City during the Tokachi-oki earthquake of May 16, 1968. (3) Northridge. The N-S component recorded at Sylmar County Hospital parking lot in Sylmar, California, during the Northridge, California earthquake of January 17, 1994. (4) Kobe. The N-S component recorded at the Kobe Japanese Meteorological Agency

station during the Hyogo-ken Nanbu earthquake of January 17, 1995. The absolute peak acceleration of the earthquake records are 3.417, 2.250, 8.2676, and 8.1782 m/sec², respectively. Moreover, various levels of each of the earthquake records including: 0.5, 1.0 and 1.5 times the magnitude of El Centro and Hachinohe; and 0.5 and 1.0 times the magnitude of Northridge and Kobe are employed. This is a total of 10 earthquake records to be considered in the evaluation of the control strategy.

To show the performance of the proposed controllers, time histories of relative displacement of the third story when the structure is subjected to the El Centro and Hachinohe earthquakes are depicted in Figs. 6 and 7 considering NNPC and NN controllers, respectively. As can be seen, the relative displacements are noticeably reduced after control action. Not only the peak responses but also the overall amplitudes are reduced in the responses.

The performance of the controller is also investigated based on the evaluation criteria ($J_1 - J_6$) specified for the nonlinear benchmark buildings (Ohtori *et al.* 2004), which are briefly presented in Table 1. These criteria are calculated as a ratio of the controlled and the uncontrolled responses.

The first three criteria are based on peak interstory drift ratio (J_1), level acceleration (J_2) and base shear (J_3), over the range $i=[1,3]$. In these expression: $d_i(t)$ is the interstory drift of the above ground level over the time history of each earthquake, h_i is the height of each of the associated stories, δ^{max} is the maximum interstory drift ratio of the uncontrolled structure, $\ddot{x}_{ai}(t)$ and \ddot{x}_a^{max} are absolute acceleration of the i -th level with and without control devices respectively, m_i is the seismic mass of the i -th above ground level and F_b^{max} is the maximum base shear of the uncontrolled structure for each respective earthquake.

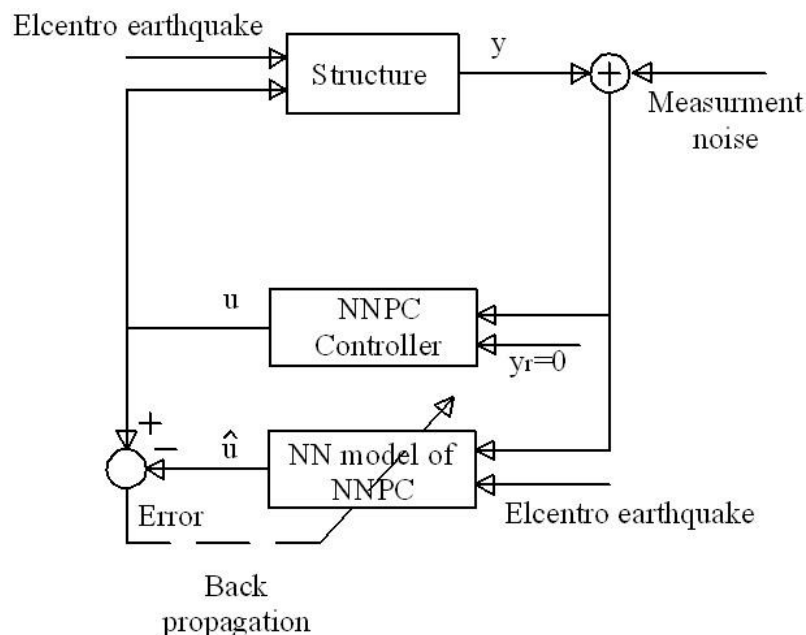


Fig. 5 Training NN controller

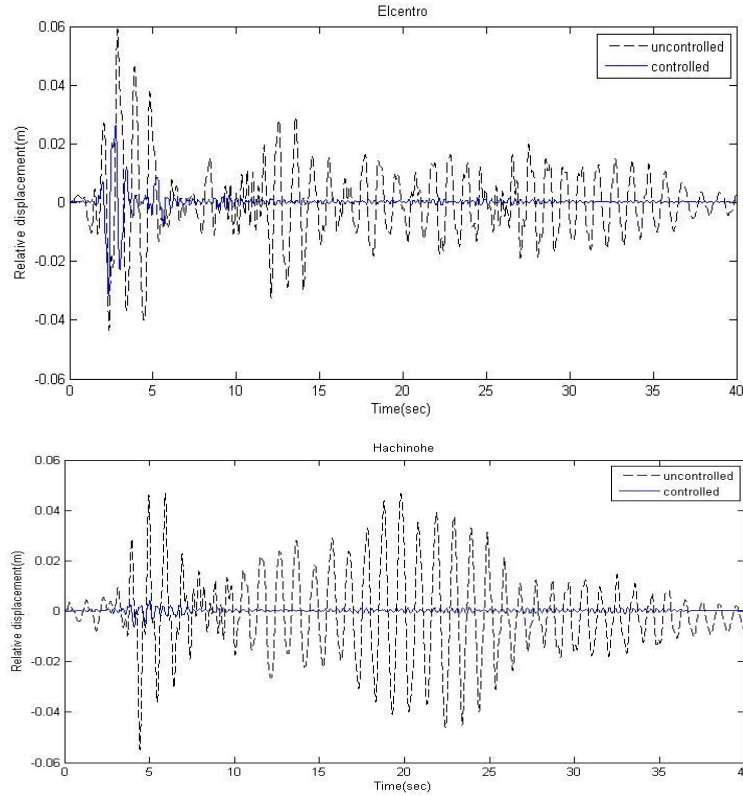


Fig. 6 Comparison of relative displacement of the 3rd_story for uncontrolled and NNPC

Table 1 Performance criteria

$J_1 = \max_{\substack{\text{El Centro} \\ \text{Hachinohe} \\ \text{Northridge} \\ \text{Kobe}}} \left\{ \frac{\max_{t_i} \frac{ d_i(t) }{h_i}}{\delta^{max}} \right\}$	$J_2 = \max_{\substack{\text{El Centro} \\ \text{Hachinohe} \\ \text{Northridge} \\ \text{Kobe}}} \left\{ \frac{\max_{t_i} \ddot{x}_{ai}(t) }{\ddot{x}_a^{max}} \right\}$ <p>Level acceleration</p>	$J_3 = \max_{\substack{\text{El Centro} \\ \text{Hachinohe} \\ \text{Northridge} \\ \text{Kobe}}} \left\{ \frac{\max_t \sum_i m_i \ddot{x}_{ai}(t) }{F_b^{max}} \right\}$ <p>Base shear</p>
Interstory drift ratio		
$J_4 = \max_{\substack{\text{El Centro} \\ \text{Hachinohe} \\ \text{Northridge} \\ \text{Kobe}}} \left\{ \frac{\max_t \frac{\ d_i(t)\ }{h_i}}{\ \delta^{max}\ } \right\}$	$J_5 = \max_{\substack{\text{El Centro} \\ \text{Hachinohe} \\ \text{Northridge} \\ \text{Kobe}}} \left\{ \frac{\max_t \ \ddot{x}_{ai}(t)\ }{\ \ddot{x}_a^{max}\ } \right\}$ <p>Normed level acceleration</p>	$J_6 = \max_{\substack{\text{El Centro} \\ \text{Hachinohe} \\ \text{Northridge} \\ \text{Kobe}}} \left\{ \frac{\ \sum_i m_i \ddot{x}_{ai}(t)\ }{\ F_b^{max}\ } \right\}$ <p>Normed base shear</p>
Normed interstory drift ratio		

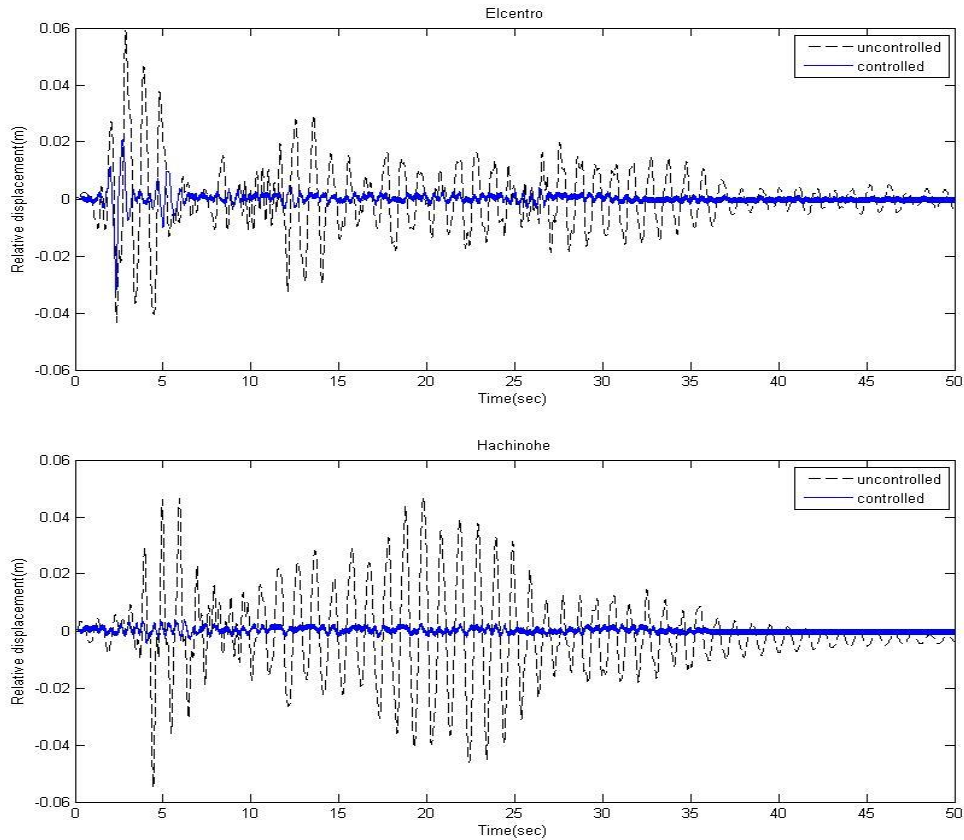


Fig. 7 Comparison of relative displacement of the 3rd_story for uncontrolled and NN Controller

The next three criteria are based on normed building responses. The interstory drift (J_4), level acceleration (J_5), and base shear (J_6) are defined in their normed based forms where the norm, $\| \cdot \|$, is computed using the following equation

$$\| \cdot \| = \sqrt{\frac{1}{t_f} \int_0^{t_f} [\cdot]^2 dt} \tag{2}$$

which t_f is a sufficiently large time to allow the response of the structure to attenuate.

Table 2 presents the evaluation criteria as the ratio of the controlled response to the uncontrolled response for each earthquake record individually for NN and LQG controllers. Here, the NN controller is designed to reduce the relative displacement and as can be seen in Table 2 it has reduced both the peak and normed drift criteria (J_1 and J_4) for all earthquake records significantly. According to this table, J_1 and J_4 are reduced 13-81% and 44-91%, respectively considering different earthquakes. Unfortunately, NN controller has increased peak and normed acceleration criteria (J_2 and J_3) especially normed acceleration for all earthquake records. Reduction of building acceleration is important in situations where occupant comfort is a high priority. A circumstance where control of acceleration takes precedent over control of drift often

arises with the design of very tall and slender buildings. In these situations other criteria can be used for optimization in the proposed control strategy instead of relative displacement or even multi objective criteria can be employed. In Table 2, J_3 and J_6 also show that the peak and normed base shear are increased in most cases. Comparing the NN and LQG controllers concludes that the NN is more successful than LQG controller in most earthquakes, considering drift criteria.

5.2 Fragility curves

One method in estimation of seismic damage in buildings and bridges and evaluation of the effects and robustness of control methods is so called fragility curves. The fragility defines the conditional probability of the seismic demand (D) placed upon the structure exceeding its capacity (C) limits for a given level of earthquake intensity (S), as shown in the following equation

$$Fragility = P[D \geq C | S] \quad (3)$$

Different methods have been used to develop fragility curves. These methods may be sub-divided into four categories based on the sources of data as: empirical, judgmental, analytical and hybrid vulnerability methods (Kwon and Elnashai 2006). In the absence of adequate empirical data, analytical methods usually have been used to develop fragility curves. In these methods, the structural demands and/or capacities used to evaluate failure probability are estimated through such methods as elastic spectral, nonlinear static and nonlinear time history analyses (Padgett and DesRoches 2008). Here, nonlinear time history analyses are used to generate fragility curves.

Table 2 Performance criteria for NNC and LQG controllers

Criteria	Controller	Erth	El	El	El	Hachin	Hachin	Hachin	North	North	Kobe	Kobe	Maxi Mum
		(Intensity)	centro (0.5)	centro (1)	centro (1.5)	ohe (0.5)	ohe (1)	ohe (1.5)	ridge (0.5)	ridge (1)			
J_1	NNC		0.19	0.61	0.87	0.13	0.14	0.22	0.41	0.78	0.62	0.86	0.87
	LQG		0.42	0.59	0.75	0.62	0.74	0.83	0.86	1.11	0.69	0.73	1.11
J_2	NNC		1.93	1.29	1.33	2.11	1.30	1.20	1.14	1.36	1.14	1.00	2.11
	LQG		0.53	0.69	0.91	0.62	0.75	0.84	0.89	1.05	0.83	0.88	1.05
J_3	NNC		0.69	1.20	1.34	0.70	0.58	0.80	0.86	1.17	1.26	1.20	1.34
	LQG		0.40	0.70	0.79	0.52	0.73	0.91	0.82	0.87	0.74	0.94	0.94
J_4	NNC		0.39	0.45	0.56	0.27	0.18	0.17	0.09	0.37	0.30	0.31	0.56
	LQG		0.45	0.48	0.50	0.32	0.35	0.99	0.50	0.67	0.26	0.32	0.99
J_5	NNC		13.01	7.71	4.56	10.13	5.99	4.76	11.05	2.42	8.46	4.90	13.01
	LQG		0.44	0.54	0.56	0.30	0.36	0.43	0.59	0.66	0.53	0.63	0.66
J_6	NNC		3.24	2.25	1.65	2.40	1.50	1.29	3.06	1.31	2.43	1.70	3.24
	LQG		0.40	0.49	0.51	0.28	0.34	0.41	0.61	0.59	0.47	0.58	0.61

When developing fragility curves, selection of representative set of earthquakes that represents the variability in seismic input is an important step. Usually the number of available and usable actual ground motion records is not sufficient to obtain the accurate results. Somerville *et al.* (1997) generated three set of 20 ground motions for the SAC project to represent ground motions having probabilities of exceedance of 50% in 50 years (corresponding to a return period of 72 years), 10% in 50 years (corresponding to a return period of 474 years), and 2% in 50 years (corresponding to a return period of 2475 years) in the Los Angeles region. These sets of ground motions are referred to as the 50 in 50 Set, 10 in 50 Set, and 2 in 50 Set, respectively. The acceleration histories have been scaled so as to conform roughly to the 1997 NEHRP design spectrum for firm soil for the specified return periods. Since Bazzurro and Cornell (1994) suggested that five to seven input motion are sufficient for representing the hazard, in this study only two sets of ground motions (2 in 50 set and 10 in 50 set) including 40 earthquakes are used as a seismic input.

Definition of limit states plays a significant role in the construction of the fragility curves. FEMA 356 (2000), defines three limit states based on inter-story drift. These limit states are the Immediate Occupancy (IO), the Life Safety (LS) and the Collapse Prevention (CP). FEMA specifies 0.7, 2.5 and 5% for the maximum inter-story drift ratio of steel moment frames associates with the IO, LS and CP limit stats, respectively.

Fig. 8 shows fragility curves for uncontrolled and controlled structure subjected to 40 ground motions considering FEMA limit states.

As it is obvious, NN controller reduces the probability of damage for a wide and common range of intensities, significantly. But, When PGA (sa) is greater than 1.3 g (2.3 g), the NN controller increases the probability of damage. Because the ground motion intensities are rarely greater than stated amount, the performance of the NN controller in damage reduction is realized, perfectly. Fig.8 shows that the performance of the controller in low intensities is better than high. This figure also shows that the NN is more effective in damage reduction than the LQG controller. Moreover, as can be seen, the NN controller is effective for a wider range of intensities than the LQG controller.

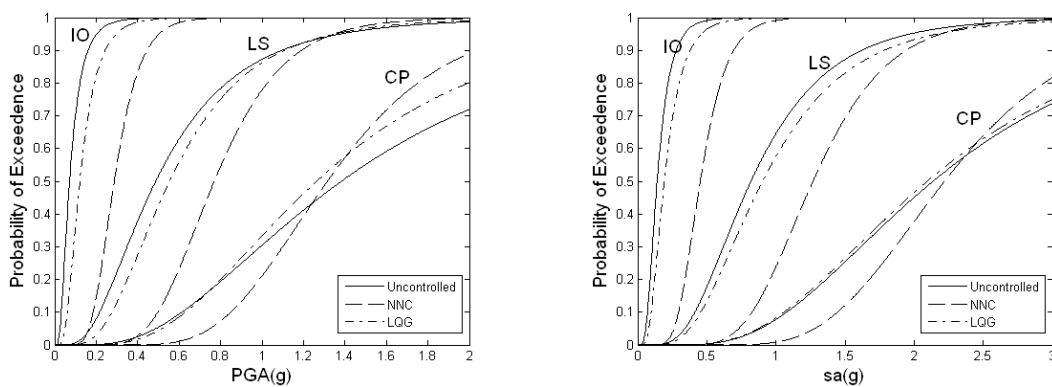


Fig. 8 Fragility curves for controlled and uncontrolled structure

6. Conclusions

In this paper active neural network predictive controller (NNPC) is used to control nonlinear structures subjected to ground excitations. A neural network model of nonlinear structure predicts future structure response. The controller then calculates the control input that will optimize a cost function over a specified future time horizon. Since the NNPC controller is very time consuming and not suitable for real-time control, NNPC controller is used to obtain the training data for a neural network (NN) controller. The effectiveness of the NNPC and NN controllers are illustrated and verified using simulated response of a 3-story full-scale, nonlinear benchmark building excited by several historical earthquake records.

Table 2 presented the evaluation criteria as the ratio of the controlled response to the uncontrolled response. The results demonstrate that the NN algorithm is quite effective in relative displacement reduction for wide range of motions from moderate to severe seismic events, compared with the LQG controller. Since here the proposed controller was designed to minimize the relative displacement, it can be concluded that the proposed control strategy has worked properly. Moreover, Table 2 showed that the proposed controller increases the acceleration response. So, in the situation that the acceleration reduction is the most important criteria such as tall buildings, other criteria or multi objective criteria can be used for optimization in the proposed control strategy. Generating fragility curves for the uncontrolled and controlled structure shows that in common ground motion intensities the proposed controller is completely effective to reduce the probability of damage.

References

- Bani-Hani, K.A., Mashal, A. and Sheban, M.A. (2006), "Semi-active neuro-control for base-isolation system using magnetorheological (MR) dampers", *Earthq. Eng. Struct. D.*, **35**, 1119-1144.
- Bazzurro, P. and Cornell, C.A. (1994), "Seismic hazard analysis of nonlinear structures I: methodology", *J. Struct. Eng.- ASCE*, **120**(11), 3320-3344.
- Camacho, E.F. and Bordons, C. (1999), *Model Predictive Control*, London: Springer.
- FEMA 356 (2000), *Prestandard and commentary for the seismic rehabilitation of buildings*, Federal Emergency Management Agency.
- Gholampour, A.A., Ghassemieh, M. and Kiani, J. (2014), "State of the art in nonlinear dynamic analysis of smart structures with SMA members", *Int. J. Eng. Sci.*, **75**, 108-117.
- Jung, H.J., Lee, H.J., Yoon, W.H., Oh, J.W. and Lee, I.W. (2004), "Semiactive neurocontrol for seismic response reduction using smart damping strategy", *J. Comput. Civil Eng.*, **18**(3), 277-280.
- Karamodin, A. and H-Kazemi, H. (2008), "Semi-active control of structures using neuro-predictive algorithm for MR dampers", *J. Struct. Control Health Monit.*, **17**(3), 237-253.
- Karamodin, A., Irani, F. and Baghban, A. (2012), "Effectiveness of a fuzzy controller on the damage index of nonlinear benchmark buildings", *Scientia Iranica A*, **19**(1), 1-10.
- Kim, B., Washington, G.N. and Yoon, H.S. (2013), "Active vibration suppression of a 1D piezoelectric bimorph structure using modelpredictive sliding mode control", *Smart Struct. Syst.*, **11**(6), 623-635.
- Kumar, R., Singh, S.P. and Chandrawat, H.N. (2007), "MIMO adaptive vibration control of smart structures with quickly varying parameters: Neural networks vs classical control approach", *J. Sound Vib.*, **307**, 639-661.
- Kwon, O.S. and Elnashai, A. (2006), "The effect of material and ground motion uncertainty on the seismic vulnerability curves of RC structure", *Eng. Struct.*, **28**, 289-303.
- Lee, H.J., Yang, Y.G., Jung, H.J., Spencer, B.F. and Lee, I.W. (2006), "Semi-active neurocontrol of a base

- isolated benchmark structure”, *Struct. Control Health Monit.*, **13**, 682-692.
- Lopez-Almansa, F., Andrade, R., Rodellar, J. and Reinhorn A.M. (1994a), “Modal predictive control of structures. I: formulation”, *J. Eng. Mech. - ASCE*, **120**(8), 1743-1760.
- Lopez-Almansa, F., Andrade, R., Rodellar, J. and Reinhorn A.M. (1994b), “Modal predictive control of structures. II: implementation”, *J. Eng. Mech. - ASCE*, **120**(8), 1761-1772.
- Lu, L.Y., Lin, C.C., Lin, G.L. and Lin, C.Y. (2010), “Experiment and analysis of a fuzzy-controlled piezoelectric seismic isolation system”, *J. Sound Vib.*, **329**, 1992-2014.
- Mei, G., Kareem, A. and Kantor, J.C. (2001), “Real-time model predictive control of structures under earthquakes”, *Earthq. Eng. Struct. D.*, **30**, 995-1019.
- Mei, G., Kareem, A. and Kantor, J.C. (2002), “Model predictive control of structures under earthquakes using acceleration feedback”, *J. Eng. Mech. - ASCE*, **128**(5), 574-585.
- Ohtori, Y., Christenson, R.E., Spencer, B.F. and Dyke, S.J. (2004), “Benchmark control problems for seismically excited nonlinear buildings”, *J. Eng. Mech. - ASCE*, **130**(4), 366-387.
- Padgett, J.E. and DesRoches, R. (2008), “Methodology for the development of analytical fragility curves for retrofitted bridges”, *Earthq. Eng. Struct. D.*, **37**, 1157-1174.
- Pourzeynali, S., Lavasani, H.H. and Modarayi, A.H. (2007), “Active control of high rise building structures using fuzzy logic and genetic Algorithms”, *Eng. Struct.*, **29**, 346-357.
- Qin, S.J. and Badgwell, T.J. (1996), “An overview of industrial model predictive control technology”, *Chemical Process Control-V Proceedings of AIChE Symposium Series 316*, **93**, 232-256.
- Reigles, D.G. and Symans, M.D. (2006), “Supervisory fuzzy control of a base-isolated benchmark building utilizing a neuro-fuzzy model of controllable fluid viscous dampers”, *Struct. Control Health Monit.*, **13**, 724-747.
- Rodellar, J., Barbat, A.H. and Sanchez, J.M. (1987), “Predictive control of structures”, *J. Eng. Mech. - ASCE*, **113**(6), 797-812.
- Sommerville, P., Smith, N., Punyamurthula, S. and Sun, J. (1997), *Development of ground motion time histories for phase II of the FEMA/SAC steel project*, SAC Background Document Report No. SAC/BD-97/04.
- Suhir, E. (2014), “Elastic stability of a compressed cantilever beam on an elastic foundation, with application to a dual-coated fiber-optic connector”, *Int. J. Eng. Sci.*, **83**, 85-94.
- Xu, L.H. and Li, Z.X. (2011), “Model predictive control strategies for protection of structures during earthquakes”, *Struct. Eng. Mech.*, **40**(2), 233-243.
- Zhang, J., He, L., Wang, E. and Gao, R. (2008), “A LQR controller design for active vibration control of flexible structures”, *Comput. Intell. Ind. Appl.*, **1**, 127-132.

